Ma, Y.; Halsall, C.J.; Xie, Z.; Koetke, D.; Mi, W.; Ebinghaus, R.; Gao, G.:
Polycyclic aromatic hydrocarbons in ocean sediments from the North Pacific to the Arctic Ocean
In: Environmental Pollution (2017) Elsevier

DOI: 10.1016/j.envpol.2017.04.087

Polycyclic Aromatic Hydrocarbons in ocean sediments from the North Pacific to the Arctic Ocean

Yuxin Ma [1], Crispin J. Halsall [2,*], Zhiyong Xie [3], Danijela Koetke [3], Wenying Mi [3], Ralf Ebinghaus[3], Guoping Gao [1,**]

[1] College of Marine Sciences, Shanghai Ocean University, Shanghai 201306, China

[2] Lancaster Environment Centre, Lancaster University, Lancaster, LA1 4YQ, UK

Department of Chemistry, Lancaster University, Lancaster, LA1 4YB, UK

[3] Helmholtz-Zentrum Geesthacht, Centre for Materials and Coastal Research GmbH, Institute of Coastal Research, Max-Planck Straße. 1, D-21502 Geesthacht, Germany

*Corresponding author. Tel.: +44-0-1524594330

E-mail: c.halsall@lancaster.ac.uk

**Corresponding author. Tel.: +86-15692160123

E-mail: gpgao@shou.edu.cn

[1] Eighteen polycyclic aromatic hydrocarbons (PAHs) were measured in surficial sediments along a marine transect from the North Pacific into the Arctic Ocean. The highest average Σ_{18}PAHs concentrations were observed along the continental slope of the Canada Basin in the Arctic (68.3 ± 8.5 ng g^{-1} dw), followed by sediments in the Chukchi Sea shelf (49.7 ± 21.2 ng g^{-1} dw) and Bering Sea (39.5 ± 11.3 ng g^{-1} dw), while the Bering Strait (16.8 ± 7.1 ng g^{-1} dw) and Central Arctic Ocean sediments (13.1 ± 9.6 ng g^{-1} dw) had relatively lower average concentrations. The use of principal components analysis with multiple linear regression (PCA/MLR) indicated that on average oil related or petrogenic sources contributed ~42% of the measured PAHs in the sediments and marked by higher concentrations of two methylnaphthalenes over the non-alkylated parent PAH, naphthalene. Wood and coal combustion contributed ~32%, and high temperature pyrogenic sources contributing ~26%. Petrogenic sources, such as oil seeps, allochthonous coal and coastally eroded material such as terrigenous sediments particularly affected the Chukchi Sea shelf and slope of the Canada Basin, while biomass and coal combustion sources appeared to have greater influence in the central Arctic Ocean, possibly due to the effects of episodic summertime forest fires.

1. Introduction

[2] Polycyclic aromatic hydrocarbons (PAHs) are carcinogenic and mutagenic pollutants originating from incomplete combustion and pyrolysis of carbonaceous materials [*Ding et al.*, 2007; *Okona-Mensah et al.*, 2005]. They have both anthropogenic and natural sources. In particular, PAHs are well established markers with the ability to trace specific sources of anthropogenic contamination (i.e. fossil fuel vs. biomass combustion) and natural inputs (i.e. oil seeps, forest fires and terrestrial debris) to marine systems [*Jaward et al.*, 2004; *Nizzetto et al.*, 2008; *Yunker et al.*, 2002a; *Yunker et al.*, 2002b]. Although PAHs represent only a small fraction (0.2–7%) of the total composition of crude oil, their relative persistence in the environment and potential toxicity to marine organisms warrants research into their sources and fate in marine systems [*Harvey et al.*, 2014].

[3] Analysis of benthic marine sediments allows the assessment of particle settling and post-depositional behavior as an important marine sink for contaminants initially present in the overlying water column [*Ma et al.*, 2015; *Yunker et al.*, 1996]. For PAHs that possess relatively high organic-carbon/water partitioning coefficients (e.g. log $K_{OC} \geq 4.5$) then their sorption to organic matter [*Dachs and Eisenreich*, 2000] and subsequent particle settling could be a significant removal process from the water column which, in part, could be driven by the settling fluxes of particle organic carbon associated with primary production by phytoplankton (i.e. the 'biological pump') [*Dachs et al.*, 2002; *Galban-Malagon et al.*, 2012]. For remote pelagic environments like the North Pacific and Arctic Oceans, then PAH input is likely to be

driven primarily by atmospheric deposition [*MacDonald et al.*, 2000]. As PAHs have been systematically monitored in ambient Arctic air at sites in Canada and the Norwegian Arctic [*Becker et al.*, 2006; *Wang et al.*, 2010], several modeling studies have indicated continental sources of PAHs via long-range transport from mid-latitudes [*Halsall et al.*, 1997; *Hung et al.*, 2005; *Sofowote et al.*, 2011; *Wang et al.*, 2010]. The observed air–sea gas exchange gradients of PAHs from North Pacific to Arctic Oceans, strongly favored net deposition trends, with increasing deposition with increasing latitude [*Ma et al.*, 2013]. However, in addition to atmospheric sources and subsequent deposition to marine surfaces, the extraction and processing of fossil fuels on the wide Arctic shelf seas and adjacent coastal areas provides a petrogenic source of PAHs to sediments [*Yunker and Macdonald*, 1995; *Yunker et al.*, 2011; *Yunker et al.*, 2002a]. Climate change perturbations are driving increased coastal erosion and permafrost thawing in the Arctic [*AMAP*, 2012], increasing the likelihood of wider dispersal of petrogenic PAHs [*McGuire et al.*, 2009], such as the offshore transport of sediment-laden ice from the coastal shelf areas and subsequent export between the shelves and the central Arctic Ocean [*Belicka and Harvey*, 2009; *Yunker et al.*, 1996]. Repeat surveys of benthic sediments along similar geographic transects on an annual or biannual basis such as the Chinese National Arctic Research Expeditions have the potential to develop a time series of pollutant concentrations. In turn the sedimentary time-series can be related to changing sources and/or changes to pollutant processing within the marine system.

[4] The aim of this study was to examine the spatial distribution of PAHs in benthic

sediments from the North Pacific to the central Arctic Ocean (via the Bering Strait) and to examine their composition using PAH ratios and statistical pattern recognition techniques in the PAH profile to infer likely sources affecting the different marine areas along this latitudinal transect.

2. Experimental Section

2.1 Sampling Cruise

[5] Marine sediment samples were collected onboard the ice-breaker R/V Xuelong (Snow Dragon) during a Chinese National Arctic Research Expedition (Table A1). Specifically, 0-2cm sediment samples were collected during the 4th Arctic expedition between July and September 2010 (CHINARE 4). The sampling stations roughly follow a latitudinal northward transect across the Bering Sea through Bering Strait and cover the Chukchi Sea, Canadian Basin and central Arctic Ocean (53-88°N). Marine sediments were collected with a stainless steel grab sampler and scooped using a pre-cleaned stainless steel scoop and placed into baked and solvent-rinsed aluminum containers. All samples were stored at -20°C until further analysis. Sediments were then carefully freeze-dried and sieved (100 mesh size sieve) before gentle grinding and homogenization.

2.2 Material and Reagents

[6] The PAH compounds (Dr. Ehrenstorfer, Germany) measured in this study were as follows (abbreviations in parentheses): naphthalene (Nap), 1-methylnaphthalene (1-MN), 2-methylnaphthalene (2-MN), acenaphthylene (Acl), acenaphthene (Ace), fluorene (Flu), phenanthrene (Phe), anthracene (Ant), fluoranthene (Fluor), pyrene

(Py), benzo[a]anthracene (BaA), chrysene (Chry), benzo[b]fluoranthene (BbF), benzo[k]fluoranthene (BkF), benzo[a]pyrene (BaP), indeno[1,2,3-cd]pyrene (InP), dibenz[a,h]anthracene (DBahA), benzo[ghi]perylene (BghiP). Neutral silica gel 80-100 mesh) and anhydrous sodium sulfate were cleaned with dichloromethane (DCM) using an MX-Soxhlet extractor for 24 h, and baked at 450°C for 12 h. Silica gel was deactivated with 10% (w:w) of precleaned deionized water (extracted with DCM). All organic solvents used were of analytical grade, and redistilled using a glass distillation system. Laboratory glassware was baked at 250 °C for 12 h, and then rinsed with acetone and *n*-hexane.

2.3 Sample Extraction and Fractionation

[7] About 10 g of sediment and 10 g Na_2SO_4 was packed in a glass column and spiked with 10 µl of 1 ng/µL surrogate standards, e.g. PAH-Mix 9 deuterated (Table A2), Soxhlet extracted with DCM for 24 h at a flow rate of 5 mL/min. Five grams of activated copper granules were added to the extraction flasks during the extraction to remove elemental sulfur. Extracts were evaporated to 1–2 mL using hexane as keeper and further cleaned on a silica column (2.5 g, 10 % water deactivated) topped on 3 g anhydrous granulated sodium sulfate. The first fraction, eluted with 20 mL *n*-hexane, was collected and concentrated down to 150 µL. 10µL of 50 pg ^{13}C–PCB 208 (Cambridge Isotope Laboratories) was added as an injection standard [*Zhong et al.*, 2012].

2.4 Instrumental Analysis

[8] The samples were analyzed with an Agilent 6890N gas chromatograph coupled to

an Agilent 5975 mass spectrometer (GC-MS) (Agilent Technologies, Avondale, PA, USA), operating in electron impact and selective ion monitoring modes (SIM), and fitted with a HP-5MS capillary column (30 m × 250 μm i.d.; 0.25 μm film thickness, J&W Scientific) for chromatographic separation. The transfer line and the ion source temperature were maintained at 280 and 230 °C, respectively. The column temperature program was initiated at 60 ºC for 2.0 min, increased to 180 °C at a rate of 30 ºC min^{-1}, and ramped at 2 °C min^{-1} to 300 °C and held for 10 min. The flow rate of the carrier gas helium was kept constant at 1.3 mL min^{-1}. The extracts (1.0 μL) were injected onto GC-MS in splitless mode with an inlet temperature of 280 °C. Quantitation was performed using the internal calibration method based on a 5-point calibration curve for individual PAHs. The response factors were derived from the calibration curves (5-points) with response ratios between target compounds (0–750 pg μL^{-1}) and the internal standard (50 pg μL^{-1}).

[9] The measurements of total organic carbon (TOC), total inorganic carbon (TIC), residual oxidizable carbon (ROC), and total carbon (TC) were conducted using temperature-dependent differentiation of total carbon on a multi-phase carbon and water analyzer (LECO RC612, St Joseph, MI, USA). The parameters were analysed sequentially: (i) TOC400: 150 °C to 400 °C at 70 °C/min (120-sec hold) in oxygen flow, (ii) TIC900: 400 °C to 900 °C at 120 °C/min (250-sec hold) in nitrogen flow, (iii) ROC: 900 °C (100-sec hold) in oxygen flow (Beuth Verlag, 2015). Total carbon was calculated as the sum of TOC400, TIC900 and ROC.

2.5 Quality Control and Quality Assurance

[10] Surrogate standards were added to all the samples to monitor matrix effects. The recoveries of target PAHs ranged from 60 ± 3% to 91 ± 7% in 5 spiked samples. The method detection limits (MDLs) were derived from the procedural blanks and quantified as mean field blanks plus three times the standard deviation (3σ) of field blanks, ranging from 0.001 ng/g for Benzo[k]fluoranthene to 0.053 ng/g for Naphthalene. Five procedural blanks were extracted together with the samples. The major PAH contamination found in the procedural blanks comprised of Nap, Phe and Py with concentrations of 0.028 ± 0.008, 0.019 ± 0.007 and 0.017 ± 0.007 ng/g, which account for < 1.1% of those compounds in the sediment samples.

3. Results and Discussion

3.1 Geographic Distribution of PAHs

[11] The total concentrations of 18 PAHs in the surface sediment (Σ_{18}PAHs, sum of the detected 16 parent PAHs and 2 alkyl-PAHs) ranged from 8.5 to 78.3 ng g^{-1} dry weight (dw), with a mean of 37.3 ± 24.0 ng g^{-1} dw during the entire cruise. To assess the spatial distribution of the PAHs, then the sampling sites were separated into five geographical areas: Bering Sea, Bering Strait, Chukchi Sea, Canadian Basin margin and Central Arctic Ocean, with a summary of the chemical concentrations for these areas presented in Table 1. The spatial distribution of Σ_{18}PAHs along the cruise tracks is shown in Figure 1. Analysis of variance (ANOVA) demonstrated significant differences in the mean concentrations between the five geographical regions.

[12] The highest average Σ_{18}PAHs concentrations were observed in the Canadian Basin margin region (68.3 ± 8.5 ng g^{-1} dw), followed by sample stations in the

Chukchi Sea (49.7 ± 21.2 ng g^{-1} dw) and Bering Sea (39.5 ± 11.3 ng g^{-1} dw), while the Bering Strait (16.8 ± 7.1 ng g^{-1} dw) and Central Arctic Ocean (13.1 ± 9.6 ng g^{-1} dw) had relatively lower average concentrations. It is noteworthy that concentrations of Σ_{18}PAHs showed a wide variability in the Chukchi Sea with high levels observed at sites SR11 (78.3 ng g^{-1} dw) and C07 (75.8 ng g^{-1} dw) in the northern Chukchi Sea shelf, as well as site BN03 in the Chukchi Sea marine bench edge (71.8 ng g^{-1} dw). While Σ_{18}PAHs was present as relatively lower levels at sites SR01 (8.8 ng g^{-1} dw) and SR04 (27.7 ng g^{-1} dw) in the southern Chukchi Sea shelf and site M02 (28.6 ng g^{-1} dw) in Chukchi Sea basin. However, in the margin edges of Canadian Basin, high Σ_{18}PAHs levels were observed at sites S26 (75.5 ng g^{-1} dw) and MS02 (70.5 ng g^{-1} dw), respectively.

[13] Compared with distributions of PAHs in the atmosphere and surface seawater in the same regions, which were also observed in the same cruise (see Ma et al., 2013), the PAH occurrence was quite different. Generally, the atmospheric PAHs over the Arctic Ocean were higher than the North Pacific Ocean due to with-in Arctic sources at the time of the cruise (Arctic summer) while a decreasing trend in concentrations in surface seawater was observed with increasing northerly latitude, possibly due to more effective biogeochemical removal processes in the water column [*Ma et al.*, 2013]. Although the observed air–sea gas exchange gradients strongly favored net deposition of PAHs, their efficient removal from surface waters and the water column via particle mediated biodegradation may reduce efficient transfer of these chemicals to benthic sediments [*Berrojalbiz et al.*, 2011; *Lohmann et al.*, 2009; *Yunker et al.*,

2002a]. In addition to atmospheric sources, petrogenic sources such as oil seeps and export of PAH-laden sediments from coastal regions to the shelf margins might also contribute to the PAHs observed in benthic sediments, particularly in the continental shelf margins of the Chuckchi Sea and Canada Basin and which is discussed further below.

[14] Compared with previous studies, the present results for the Chukchi Sea sediments are about 5-fold lower than PAH measurements conducted in the northeastern Chukchi Sea, Canadian Beaufort Sea and Barents Sea, including both specific parent and alkyl PAHs [*Harvey et al.*, 2014; *Yunker et al.*, 1996]. However, our data for sediments collected on the continental slope of Canadian Basin were comparable to PAH measurements conducted on sediments collected from the Chukchi Sea slope area, while for the central Arctic ocean, our results are also comparable to concentrations obtained in the Makarov Basin, but about 10-fold lower than those in Amundsen and Nansen Basin [*Yunker et al.*, 2011].

[15] The TOC composition in these surficial sediments (Table A1), displayed higher levels in the shelf regions such as the Bering Strait (average value of 0.64%) and Chukchi Sea (average value of 0.60%), and decreased towards the Bering Sea (average value of 0.43%), Canadian Basin margin region (average value of 0.27%), and the central Arctic Ocean (average value of 0.10%). Moreover, correlations were weak but still statistically significant between Σ_{18}PAHs and TOC for the entire cruise (r^2=0.367, $p<0.05$, n=30). However, no significant correlations were observed between PAHs and TOC in other Arctic regions by Yunker et al. (2011). For persistent

organic pollutants (POPs), such as PCBs, weak or insignificant relationships were obtained between TOC and these chemicals [*Ma et al.*, 2015]. It is noteworthy that sedimentation rates varied across the study transect, with high rates occurring in the northern Bering and Chukchi Seas in contrast to much lower sedimentation rates in the Canada Basin and central Arctic Ocean [*Darby et al.*, 2009]. The seasonally ice-covered Bering Strait and Chukchi Seas represent waters with exceptional productivity and the subsequent large particle fluxes due to the "biological pump" over these shallow shelf regions will serve to efficiently export organic matter present in the water column to the underlying sediment [*Grebmeier et al.*, 2006]. Relatively lower rates of primary production over the Canada Basin and central Arctic Ocean result in much lower vertical fluxes of organic matter in the water column and corresponding sedimentation rates [*Darby et al.*, 2009]. Primary productivity in these deeper water regions maybe further impeded in a warmer Arctic with less ice [*Cai et al.*, 2010]. The surficial sediment samples (collected to a depth of 2 cm) therefore represent sediment that has accumulated over different time periods. Higher sedimentation rate regions yielding sediments comprising of material that has accumulated over the last few decades, in contrast to material in the lower accumulation regions that represents accumulation over 100s of years and hence representing time periods when PAH sources and input to the deep ocean environment may have changed considerably. Additionally, although some PAHs reached the deeper-water or ocean sediment together with organic matter, some were lost through the water column during snow/ice-melt or bio-degraded by zooplankton as discussed

above. Thus TOC might not be a strong predictor for PAH concentrations in remote oceans.

3.2 PAHs Composition

[16] Generally, the lighter PAHs such as Nap, its alkylated derivates (1-MN and 2-MN), and Phe, with average concentrations ranging 4–6 ng g^{-1} dw, were the most abundant PAHs in the sediments along the cruise, and contributed >50% to Σ_{18}PAHs. The higher MW PAHs such as Chry, BbF and BghiP, had lower concentrations of 2–3 ng g^{-1} dw. Levels of other detected PAHs were even lower, with average concentrations ≤1 ng g^{-1} dw. Moreover, although only two alkyl-PAHs were measured in this study (1-MN and 2-MN), they were more abundant than their parent PAH (Nap) at all locations along the cruise (Figure 2). Previous studies indicate that the alkyl-substituted PAHs in sediment are likely derived from petrogenic inputs and this dominance of alkyl-PAHs has been previously reported in sediments collected from the northeastern Chukchi and Beaufort Sea shelves [*Harvey et al.*, 2014; *Yunker et al.*, 1996].

[17] The PAH profile observed in surface seawater and boundary-layer air over the same oceanic transect was dominated by the lower MW PAHs, with 2-MN, Phe and Py contributing about 50% to the dissolved $\Sigma_{18}[PAHs]_{wat}$ in the seawater. However, concentrations of atmospheric heavier 5-6 ringed PAHs, which were mainly detected in the particulate phase, were quite low, while their levels were extremely low in surface seawater [*Ma et al.*, 2013]. Therefore, similarities in the PAH profile between the atmosphere, surface seawater and benthic sediments are apparent for the low MW

PAHs only, although it is difficult to ascertain the influence of atmospheric sources on the PAHs present in benthic sediments, especially given water column 'processing' prior to particle settling [*Harvey et al.*, 2014].

3.3 Source Identification by MDR

[18] Two different molecular diagnostic ratios (MDR) were calculated to estimate the influence of potential sources for the PAHs present in the sediment. The ratios of Fluor/(Fluor + Py) and InP/(BghiP + InP) in the surface sediment along the cruise tracks ranged from 0.26 to 0.57 and from 0.14 to 0.61, respectively, suggesting a well-mixed source profile of petrogenic, petrogenic combustion, as well as biomass and coal combustion origin (Figure 3-a). Similarly, a well-mixed source profile was also demonstrated for surface seawater from the North Pacific to the Arctic Ocean by MDR, however, MDR applied to the boundary-layer air of the same region indicated combustion of biomass or coal only as the principle sources of PAHs [*Ma et al.*, 2013]. MDRs however should be interpreted with some caution due to different environmental processing of the isomers during atmospheric transport [*Galarneau*, 2008] and MDRs calculated here provide a relative assessment between the various marine compartments. They demonstrate that part of the PAH component in the sediments, surface seawater and atmosphere share the same source profile, which to some extent might be due to air-sea gas exchange and subsequent transfer through the water column, although differences in the MDR indicate a degree of 'uncoupling' between these compartments..

[19] Specifically, in the sediments of Bering Sea, the ratios of Fluor/(Fluor + Py) and

277 InP/(BghiP + InP) were <0.4 and 0.2 respectively, indicating a petrogenic source
278 (Figure 3-b). While for the Chukchi Sea shelf and slope of the Canadian Basin region,
279 Fluor/(Fluor + Py) and InP/(BghiP + InP) were higher and ranged from 0.39-0.48 and
280 0.19-0.34 respectively, indicating mixing sources of petrogenic-derived and petroleum
281 combustion-derived PAHs (Figure 3-c). The dominance of the alkyl PAHs (1-MN and
282 2-MN) also support the petrogenic influence on the PAHs observed in these sediments
283 (Figure 2). The Chukchi Sea, for example, is estimated to contain 15 billion barrels of
284 recoverable oil, with potential for this region to serve as a significant source of oil and
285 natural gas in the future given that drilling rights have now been permitted [*Harvey et*
286 *al.*, 2014]. PAH petrogenic markers might originate in oil from natural occurring
287 seeps on the Chukchi shelf, although this petrogenic signal might be localized and not
288 extend to sediments in the continental shelf regions of the Canada Basin or central
289 Arctic Ocean [*Gautier et al.*, 2009]. In addition, coastal terrestrially–derived PAHs
290 might contribute to the sedimentary PAH profile in the Chukchi Sea shelf region and
291 margins of the continental shelf. The organic-rich peat, shales, bitumens and coals that
292 cover Alaska's North Slope tundra provide likely sources of alkyl-PAHs, with
293 transport of particle matter over long distances via turbidity currents or ice rafting of
294 sediments [*Jones and Yu*, 2010]. Similarly, the Mackenzie River might supply
295 elevated concentrations of alkyl-PAHs through the delivery of eroded bitumen from
296 the watershed to the Canadian shelf [*Yunker et al.*, 2002b; *Yunker et al.*, 1996], a
297 process that could be exacerbated by climate change in the Arctic [*McGuire et al.*,
298 2009].

[20] For several sample sites in the central Arctic Ocean, it is noteworthy that observed ratios of Fluor/(Fluor + Py) and InP/(BghiP + InP) indicate biomass combustion sources (Figure 3-d). Moreover, the contribution of parent PAH relative to alkyl-PAHs (ratio of Nap/(1-MN + 2-MN)) increased significantly in the central Arctic Ocean (Figure 2). To some extent, this suggests increasing import of parent PAHs on sedimentary PAHs in the central Arctic Ocean. Combustion PAH emissions from forest and prairie fires are dominated by parent PAHs which are transported atmospherically, as well as by the movement of sea and river ice with ice-associated particle matter [*Gelinas et al.*, 2001; *Schmidt and Noack*, 2000; *Yunker et al.*, 2002b]. During the CHINARE 2010 cruise, a clear increase of atmospheric PAHs, especially particle-bound PAHs, was observed in the central Arctic Ocean region, and attributed to forest fires in sub-Arctic regions of Alaska, Canada, Russia and Siberia during summer [*Ma et al.*, 2013]. From our results, these episodic inputs of pyrogenic PAHs appear to contribute to the PAHs present in the deep ocean sediments of the central Arctic Ocean, although significant PAH 'weathering' is likely to occur between the marine/atmosphere interface and the deep ocean sediments. The use of PAH ratios as source markers is limited once environmental weathering processes (chemical and biological) preferentially degrade/remove one PAH relative to another [*Galarneau*, 2008].

3.4 Source Apportionment Pattern Recognition and Multiple Linear Regression

[21] In order to have a quantitative understanding of the contributions of different PAHs sources, principal component analysis (PCA) followed by multiple linear

321 regression (MLR) of the data was used as the source apportionment method.
322 Specifically, the purpose of PCA is to represent the total variability of the original
323 PAH data in a minimum number of factors. Generally, three significant factors were
324 determined, which accounted for 88% of the total variability in the PAH dataset
325 (Table 3). The first factor was responsible for 32% of the total variance and heavily
326 weighted by Fluor, Py, Flu, BaP and BaA. This profile is indicative of wood and coal
327 combustion. Several authors report some of the lower MW PAHs like Fluor, Py and
328 Flu as predominantly indicative of low to medium temperature combustion,
329 associated with biomass combustion such as wood, but also coal combustion as a
330 fossil fuel [*Harrison et al.*, 1996; *Simcik et al.*, 1999]. The second factor was
331 responsible for 29% of the total variance. This factor was predominately composed of
332 Nap, 1-MN, 2-MN, Ace and Phe. These low MW PAHs in addition to the presence of
333 alkyl-PAHs indicate that this factor was mainly dependent on oil related sources
334 [*Larsen and Baker*, 2003; *Yunker et al.*, 1996]. The third factor accounted for 27% of
335 the total variance and was predominately weighted by the higher MW PAHs such as
336 IP, DBahA, BghiP BbF and BkF. These 5-6 ringed PAHs are mainly attributed to
337 high temperature pyrogenic sources such as liquid fossil fuels [*Larsen and Baker*,
338 2003; *Venkataraman et al.*, 1994].

339 [22] The goal of performing PCA/MLR is to determine the percent contribution of
340 different PAH sources to the sediments of the entire cruise. The detailed procedure of
341 PCA/MLR analysis was followed as previously reported by [*Larsen and Baker*, 2003].
342 The basic equation of a multiple linear model is

$$y = \sum a_i X_i + b \quad (1)$$

In this study, PCA factor scores with non-colinearity were selected as the independent variables, *Xi*. While the dependent variable, *Y*, is the standardized normal deviates of Σ_{18}PAHs. When the variables of equation 1 are normalized, the regression coefficients are represented as *A*, and the intercept *b* is 0. Then the normalized multiple linear model is

$$Y = \sum A_i X_i \quad (2)$$

Then the MLR analysis was performed stepwise using SPSS software as previously reported. Factor scores 1-3 representing wood and coal combustion, oil, high temperature pyrogenic sources, respectively, were regressed against the standard normalized deviate *Y* of the sum of 18 PAHs. The resulting equation is

$$Y = 0.543 \times FS_1 + 0.715 \times FS_2 + 0.432 \times FS_3 (R^2 = 0.99) \quad (3)$$

Here FS_1-FS_3 is the factor scores 1-3. And the calculation of the mean percent contribution is

$$\text{Mean contribution of source i (\%)} = 100 * (Ai / \Sigma Ai) \quad (4)$$

Thus, the mean percent contribution is 42.3% for the oil related sources, 32.1% for the wood and coal combustion sources, and 24% for the high temperature pyrogenic sources. It is noteworthy that the oil-related sources contributed to nearly half of the PAHs in the surficial sediments collected along the cruise transect, demonstrating that natural/petrogenic sources were important for the PAHs present in these remote ocean sediments, and indicating a degree of 'uncoupling' between the broad combustion-derived PAHs in the atmosphere and those present in benthic sediments.

4. Concluding Remarks

[23] This study provides insight into the PAH concentrations and composition in remote marine sediments in a transect that is relatively heterogenous with regards to the varied depth that the sediments were collected from i.e. shallow continental-shelf seas *vs.* deep ocean environments, and the rate of sedimentation. The evidence supporting the role played by petrogenic sources is based on examining 18 PAHs and a more extensive set of analytes including alkanes, tricyclic terpane, sterane and hopane as biomarkers would be useful alongside a wider set of alkylated-PAHs to help distinguish specific source categories such as weathered oil, coal and eroded terrigenous material. Nonetheless, in comparison to our earlier study that examined the same PAHs in air and surface seawater along broadly the same transect [*Ma et al.*, 2013], there are notable differences in the PAH profile between these 'surface' compartments and the sediments measured here. Notably the ratios of Fluo/Pyr and InP/BghiP are markedly lower in the sediments of the Chukchi Sea shelf and continental slope of the Canada Basin compared to air and surface water, supporting the petrogenic nature of the PAHs in these sediments. Furthermore, our findings that the PAHs in the sediments of the central Arctic Ocean are dominated by non-fossil fuel combustion sources is supported by the study of Yunker et al. (2011) who noted that the ubiquitous occurrence of allochthonous coal in surficial sediments made source attribution from other petrogenic sources (and probably other sources as well) difficult to determine.

[24] **Acknowledgement.** We wish to express our sincere gratitude to all the members of the 4th Chinese National Arctic Research Expedition. The research is supported by Youth Fund of National Natural Science Foundation of China (41506215) and Shanghai Sailing Program (15YF1405100). We acknowledge support from the UK NERC grant NE/E00511X/1 'ArcPOP' and EU FP7 project 'ArcRisk' (Contract no. 226534). The samples were supported by the Polar Sediment Sample Chamber of China. The sample analysis was carried out at Helmholtz-Zentrum Geesthacht, Centre for Materials and Coastal Research GmbH (HZG) and supported by the General Program of National Natural Science Foundation of China (41276197) and the Global Change Research Program of China (2015CB953900). All data generated from this study will be stored in Shanghai Ocean University's data archive, HZG's Publication archive as well as Lancaster University's Publication & Research (PURE) archive and can be obtained by contacting either YM (xinxin0709@126.com), ZX(zhiyong.xie@hzg.de) or CJH (c.halsall@lancaster.ac.uk).

Appendix: Auxiliary Materials

Auxiliary data associated with this article can be found in the Appendix: Auxiliary Materials.

Reference

AMAP (2012), Arctic Climate Issues 2011: Changes in Arctic Snow, Water, Ice and Permafrost. SWIPA Overview Report., edited by A. M. a. A. P. (AMAP), p. xi + 97pp, Oslo.

Becker, S., et al. (2006), Resolving the long-term trends of polycyclic aromatic hydrocarbons in the Canadian Arctic atmosphere, *Environ Sci Technol*, *40*(10), 3217-3222.

Belicka, L. L., and H. R. Harvey (2009), The sequestration of terrestrial organic carbon in Arctic Ocean sediments: A comparison of methods and implications for regional carbon budgets, *Geochim Cosmochim Ac*, *73*(20), 6231-6248.

Berrojalbiz, N., J. Dachs, M. J. Ojeda, M. C. Valle, J. Castro-Jimenez, J. Wollgast, M. Ghiani, G. Hanke, and J. M. Zaldivar (2011), Biogeochemical and physical controls on concentrations of polycyclic aromatic hydrocarbons in water and plankton of the Mediterranean and Black Seas, *Global Biogeochem Cy*, *25*.

Cai, W. J., L. Q. Chen, and B. S. Chen (2010), Decrease in the CO_2 uptake capacity in an ice-free Arctic Ocean basin., *Science*, *329*(5991), 556-559.

Dachs, J., and S. J. Eisenreich (2000), Adsorption onto aerosol soot carbon dominates gas-particle partitioning of polycyclic aromatic hydrocarbons, *Environ Sci Technol*, *34*(17), 3690-3697.

Dachs, J., R. Lohmann, W. A. Ockenden, L. Mejanelle, S. J. Eisenreich, and K. C. Jones (2002), Oceanic biogeochemical controls on global dynamics of persistent organic pollutants, *Environ Sci Technol*, *36*(20), 4229-4237.

Darby, D. A., J. Ortiz, L. Polyak, S. Lund, M. Jakobsson, and R. A. Woodgate (2009), The role of currents and sea ice in both slowly deposited central Arctic and rapidly deposited Chukchi-Alaskan margin sediments, *Global Planet Change*, *68*(1-2), 56-70.

Ding, X., X. M. Wang, Z. Q. Xie, C. H. Xiang, B. X. Mai, L. G. Sun, M. Zheng, G. Y. Sheng, J. M. Fu, and U. Poschl (2007), Atmospheric polycyclic aromatic hydrocarbons observed over the North Pacific Ocean and the Arctic area: Spatial distribution and source identification, *Atmos Environ*, *41*(10), 2061-2072.

Galarneau, E. (2008), Source specificity and atmospheric processing of airborne PAHs: Implications for source apportionment, *Atmos Environ*, *42*(35), 8139-8149.

Galban-Malagon, C., N. Berrojalbiz, M. J. Ojeda, and J. Dachs (2012), The oceanic biological pump modulates the atmospheric transport of persistent organic pollutants to the Arctic, *Nat Commun*, *3*.

Gautier, D. L., et al. (2009), Assessment of Undiscovered Oil and Gas in the Arctic, *Science*, *324*(5931), 1175-1179.

Gelinas, Y., K. M. Prentice, J. A. Baldock, and J. I. Hedges (2001), An improved thermal oxidation method for the quantification of soot/graphitic black carbon in sediments and soils, *Environ Sci Technol*, *35*(17), 3519-3525.

Grebmeier, J. M., L. W. Cooper, H. M. Feder, and B. I. Sirenko (2006), Ecosystem dynamics of the Pacific-influenced Northern Bering and Chukchi Seas in the Amerasian Arctic, *Prog Oceanogr*, *71*(2-4), 331-361.

Halsall, C. J., L. A. Barrie, P. Fellin, D. C. G. Muir, B. N. Billeck, L. Lockhart, F. Y. Rovinsky, E. Y. Kononov, and B. Pastukhov (1997), Spatial and temporal variation of polycyclic aromatic hydrocarbons in the Arctic atmosphere, *Environ Sci Technol*, *31*(12), 3593-3599.

Harrison, R. M., D. J. T. Smith, and L. Luhana (1996), Source apportionment of atmospheric polycyclic aromatic hydrocarbons collected from an urban location in Birmingham, UK, *Environ Sci Technol*, *30*(3), 825-832.

Harvey, H. R., K. A. Taylor, H. V. Pie, and C. L. Mitchelmore (2014), Polycyclic aromatic and aliphatic hydrocarbons in Chukchi Sea biota and sediments and their toxicological response in the Arctic cod, Boreogadus saida, *Deep-Sea Res Pt Ii*, *102*, 32-55.

Hung, H., et al. (2005), Temporal and spatial variabilities of atmospheric polychlorinated biphenyls (PCBs), organochlorine (OC) pesticides and polycyclic aromatic hydrocarbons (PAHs) in the Canadian Arctic: Results from a decade of monitoring, *Sci Total Environ*, *342*(1-3), 119-144.

Jaward, F. M., J. L. Barber, K. Booij, and K. C. Jones (2004), Spatial distribution of atmospheric PAHs and PCNs along a north-south Atlantic transect, *Environ Pollut*, *132*(1), 173-181.

Jones, M. C., and Z. Yu (2010), Rapid deglacial and early Holocene expansion of peatlands in Alaska, *Proc.Natl.Acad.Sci.*, *107*(16), 7347-7352.

Larsen, R. K., and J. E. Baker (2003), Source Apportionment of Polycyclic Aromatic Hydrocarbons in the Urban Atmosphere: A Comparison of Three Methods, *Environ. Sci. Technol*, *37*(9), 1873-1881.

Lohmann, R., R. Gioia, K. C. Jones, L. Nizzetto, C. Temme, Z. Xie, D. Schulz-Bull, I. Hand, E. Morgan, and L. Jantunen (2009), Organochlorine Pesticides and PAHs in the Surface Water and Atmosphere of the North Atlantic and Arctic Ocean, *Environ Sci Technol*, *43*(15), 5633-5639.

Ma, Y. X., Z. Y. Xie, H. Z. Yang, A. Moller, C. Halsall, M. H. Cai, R. Sturm, and R. Ebinghaus (2013), Deposition of polycyclic aromatic hydrocarbons in the North Pacific and the Arctic, *J Geophys Res-Atmos*, *118*(11), 5822-5829.

Ma, Y. X., C. J. Halsall, J. D. Crosse, C. Graf, M. H. Cai, J. F. He, G. P. Gao, and K. Jones (2015), Persistent organic pollutants in ocean sediments from the North Pacific to the Arctic Ocean, *Journal of Geophysical Research-Oceans*, *120*(4), 2723-2735.

MacDonald, R. W., et al. (2000), Contaminants in the Canadian Arctic: 5 years of progress in understanding sources, occurrence and pathways, *Sci Total Environ*, *254*(2-3), 93-234.

McGuire, A. D., L. G. Anderson, T. R. Christensen, S. Dallimore, L. D. Guo, D. J. Hayes, M. Heimann, T. D. Lorenson, R. W. Macdonald, and N. Roulet (2009), Sensitivity of the carbon cycle in the Arctic to climate change, *Ecol Monogr*, *79*(4), 523-555.

Nizzetto, L., R. Lohmann, R. Gioia, A. Jahnke, C. Temme, J. Dachs, P. Herckes, A. Di Guardo, and K. C. Jones (2008), PAHs in air and seawater along a North-South Atlantic transect: Trends, processes and possible sources, *Environ Sci Technol*, *42*(5), 1580-1585.

Okona-Mensah, K. B., J. Battershill, A. Boobis, and R. Fielder (2005), An approach to investigating the importance of high potency polycyclic aromatic hydrocarbons (PAHs) in the induction of lung cancer by air pollution, *Food Chem Toxicol*, *43*(7), 1103-1116.

Schmidt, M. W. I., and A. G. Noack (2000), Black carbon in soils and sediments: Analysis, distribution, implications, and current challenges, *Global Biogeochem Cy*, *14*(3), 777-793.

Simcik, M. F., S. J. Eisenreich, and P. J. Lioy (1999), Source apportionment and source/sink relationships of PAHs in the coastal atmosphere of Chicago and Lake Michigan, *Atmos Environ*, *33*(30), 5071-5079.

Sofowote, U. M., H. Hung, A. K. Rastogi, J. N. Westgate, P. F. Deluca, Y. S. Su, and B. E. McCarry (2011), Assessing the long-range transport of PAH to a sub-Arctic site using positive matrix factorization and potential source contribution function, *Atmos Environ*, *45*(4), 967-976.

Venkataraman, C., J. M. Lyons, and S. K. Friedlander (1994), SIRE DISTRIBUTIONS OF POLYCYCLIC AROMATIC-HYDROCARBONS AND ELEMENTAL CARBON .1. SAMPLING, MEASUREMENT METHODS, AND SOURCE CHARACTERIZATION, *Environ Sci Technol*, *28*(4), 555-562.

Wang, R., S. Tao, B. Wang, Y. Yang, C. Lang, Y. X. Zhang, J. Hu, J. M. Ma, and H. Hung (2010), Sources and Pathways of Polycyclic Aromatic Hydrocarbons Transported to Alert, the Canadian High Arctic,

Environ Sci Technol, *44*(3), 1017-1022.
Yunker, M. B., and R. W. Macdonald (1995), Composition and Origins of Polycyclic Aromatic-Hydrocarbons in the Mackenzie River and on the Beaufort Sea Shelf, *Arctic*, *48*(2), 118-129.
Yunker, M. B., R. W. Macdonald, L. R. Snowdon, and B. R. Fowler (2011), Alkane and PAH biomarkers as tracers of terrigenous organic carbon in Arctic Ocean sediments, *Org Geochem*, *42*(9), 1109-1146.
Yunker, M. B., S. M. Backus, E. Graf Pannatier, D. S. Jeffries, and R. W. Macdonald (2002a), Sources and significance of alkane and PAH hydrocarbons in Canadian arctic rivers, *Estuar Coast Shelf S*, *55*(1), 1-31.
Yunker, M. B., R. W. Macdonald, R. Vingarzan, R. H. Mitchell, D. Goyette, and S. Sylvestre (2002b), PAHs in the Fraser River basin: a critical appraisal of PAH ratios as indicators of PAH source and composition, *Org Geochem*, *33*(4), 489-515.
Yunker, M. B., L. R. Snowdon, R. W. MacDonald, J. N. Smith, M. G. Fowler, D. N. Skibo, F. A. McLaughlin, A. I. Danyushevskaya, V. I. Petrova, and G. I. Ivanov (1996), Polycyclic aromatic hydrocarbon composition and potential sources for sediment samples from the Beaufort and Barents Seas, *Environ Sci Technol*, *30*(4), 1310-1320.
Zhong, G. C., Z. Y. Xie, M. H. Cai, A. Moller, R. Sturm, J. H. Tang, G. Zhang, J. F. He, and R. Ebinghaus (2012), Distribution and Air-Sea Exchange of Current-Use Pesticides (CUPs) from East Asia to the High Arctic Ocean, *Environ Sci Technol*, *46*(1), 259-267.

Figure Captions

Figure 1. Concentrations of PAHs (Σ_{18}[PAHs]) in the surface marine sediment along the sampling cruise.

Figure 2. Contributions of Nap, 1-MN & 2-MN, other 2-3 ring PAH and 4-6 ring PAH to the ΣPAH in the five geographical regions.

Figure 3. Ratios of InP/(BghiP+InP) vs. Fluor/(Fluor+Py) in surface sediment along the cruise (a), in Bering Sea (b), Chukchi Sea shelf and slope of the Canadian Basin (c) and in the central Arctic Ocean (d).

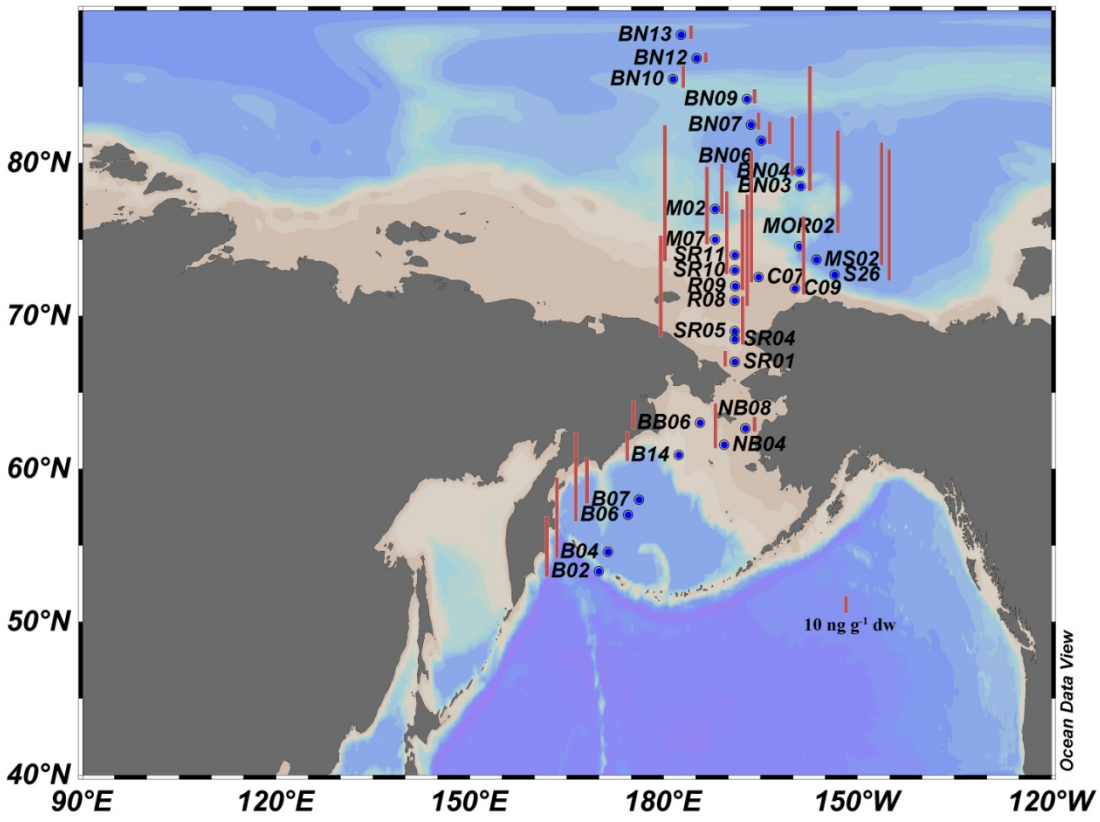

Figure 1.

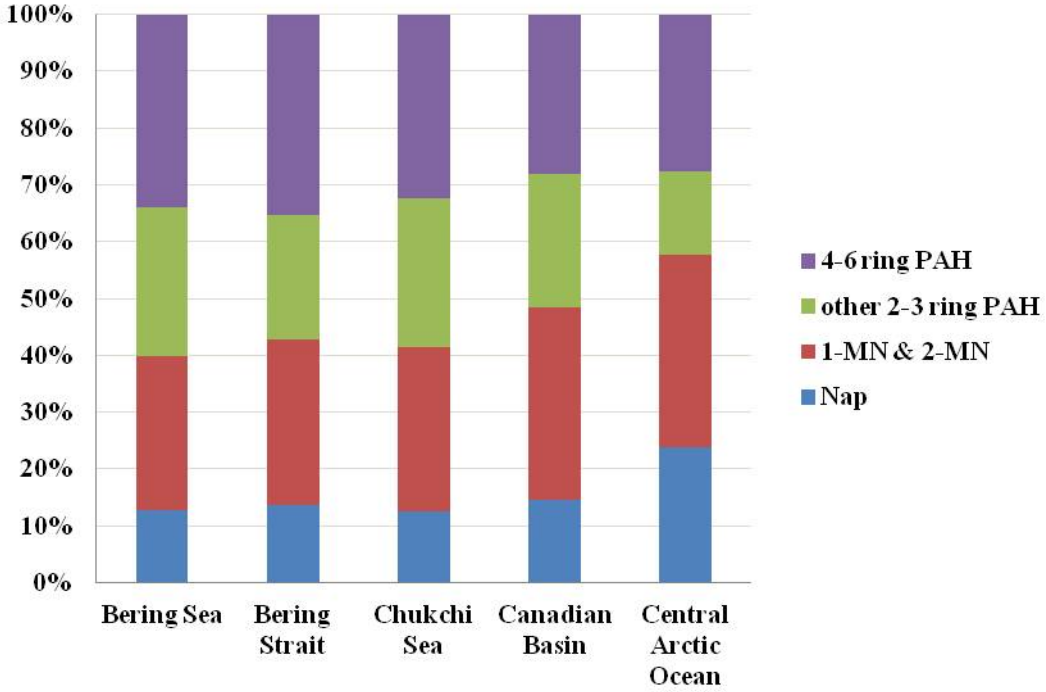

522

523 **Figure 2.**

524

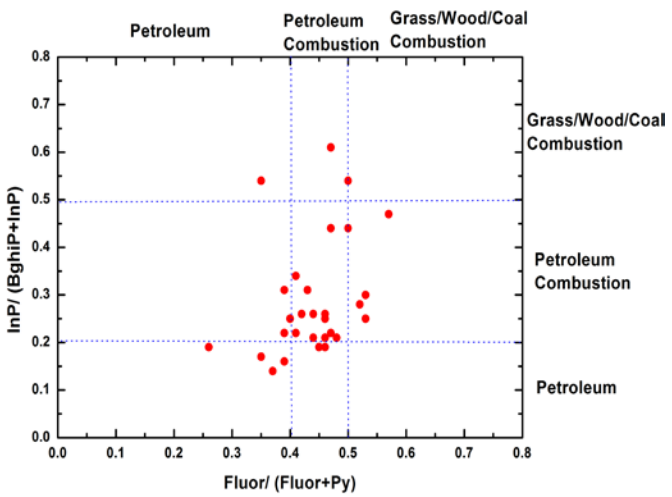

525 **a**

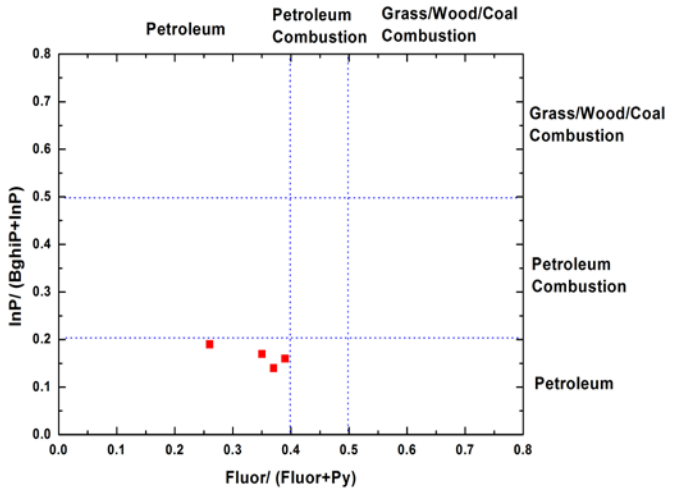

526 **b**

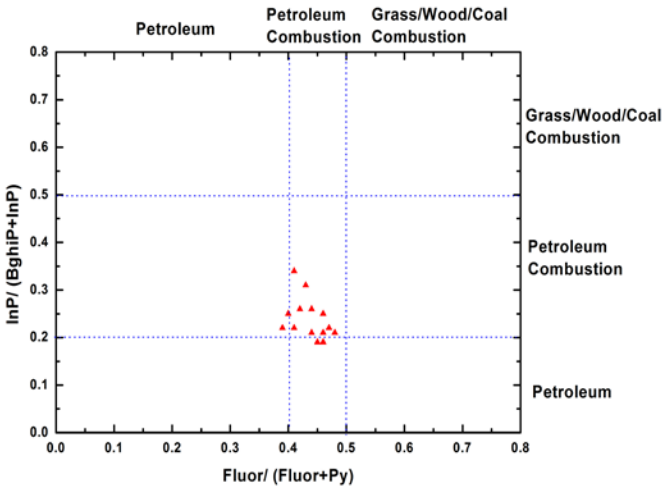

527 **c**

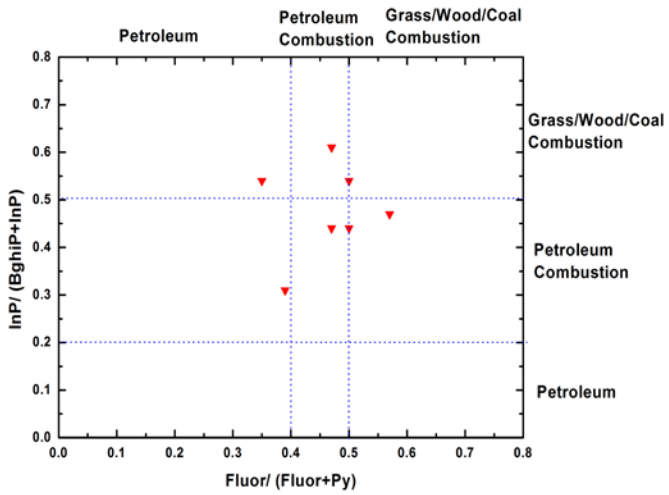

528 **d**

529 **Figure 3.**

Table 1. Concentrations of PAHs in the surface sediment (ng g^{-1} d.w.) at sampling sites from the Bering Sea to the Central Arctic Ocean

Location	Site	Nap	2-MN	1-MN	Acl	Ace	Flu	Phe	Ant	Fluor	Py
Bering Sea	B02	5.66	7.55	4.27	0.06	0.37	0.59	5.43	0.13	0.70	2.02
Bering Sea	B04	3.82	6.71	4.05	0.11	0.56	1.41	8.92	0.20	1.72	2.97
Bering Sea	B06	5.91	6.67	4.62	0.13	0.74	1.74	10.64	0.25	1.94	3.08
Bering Sea	B07	4.82	5.74	3.35	0.05	0.27	0.47	4.35	0.07	0.59	1.09
Average		5.05	6.67	4.07	0.09	0.48	1.05	7.34	0.16	1.24	2.29
Bering Strait	B14	2.21	2.17	1.28	0.02	0.14	0.32	2.34	0.10	0.89	0.79
Bering Strait	BB06	2.07	2.67	1.71	0.03	0.17	0.48	2.62	0.11	0.89	0.77
Bering Strait	NB04	3.99	5.40	3.09	0.04	0.24	0.55	3.12	0.14	0.97	0.91
Bering Strait	NB08	0.92	2.08	1.13	0.02	0.09	0.18	1.05	0.05	0.21	0.25
Average		2.30	3.08	1.80	0.03	0.16	0.38	2.28	0.10	0.74	0.68
Chukchi Sea Shelf	SR01	0.82	1.02	0.67	0.02	0.09	0.24	1.86	0.07	0.39	0.46
Chukchi Sea Shelf	SR04	2.83	4.14	2.85	0.06	0.37	0.81	5.74	0.21	1.21	1.35
Chukchi Sea Shelf	SR05	11.83	13.60	8.26	0.12	0.73	1.43	7.48	0.32	1.68	1.91
Chukchi Sea Shelf	R08	7.36	10.52	8.12	0.17	1.08	1.23	13.23	0.40	2.70	2.96
Chukchi Sea Shelf	R09	6.73	8.47	5.98	0.11	0.73	1.11	7.52	0.28	1.80	2.08
Chukchi Sea Shelf	SR10	7.50	10.18	6.34	0.11	0.65	1.12	5.79	0.22	1.62	1.92
Chukchi Sea Shelf	SR11	6.47	10.62	7.91	0.17	1.21	1.85	15.75	0.33	3.31	5.08
Chukchi Sea Shelf	C07	8.58	12.14	8.30	0.17	1.02	1.54	11.75	11.48	2.43	2.96
Chukchi Sea Shelf	C09	6.08	8.51	5.74	0.12	0.69	1.05	5.53	0.25	1.72	2.21
Chukchi Sea Shelf	M07	6.56	9.14	5.69	0.08	0.63	0.59	10.07	0.09	1.01	1.34
Chukchi Sea Basin	M02	4.47	5.28	3.48	0.05	0.28	0.36	6.14	0.04	0.57	0.79
Chukchi Sea marine bench edge	BN03	5.77	8.87	6.35	0.14	0.68	0.50	9.63	0.12	1.76	2.52
Average		6.25	8.54	5.81	0.11	0.68	0.99	8.38	1.15	1.68	2.13
Northwind ridges	MOR02	6.52	8.90	6.42	0.12	0.46	0.42	9.27	0.11	1.28	1.96
Canadian Basin	MS02	12.23	16.02	10.28	0.14	0.87	0.81	12.09	0.14	1.38	2.00
Canadian Basin	S26	10.94	16.85	10.97	0.15	1.27	1.32	16.74	0.15	1.53	1.98
Average		9.90	13.93	9.22	0.14	0.87	0.85	12.70	0.13	1.40	1.98
Central Arctic Ocean	BN04	6.10	5.55	3.15	0.05	0.23	0.24	4.37	0.06	0.53	0.82
Central Arctic Ocean	BN06	3.39	3.59	1.76	0.04	0.13	0.15	1.25	0.04	0.17	0.30
Central Arctic Ocean	BN07	3.07	2.77	1.43	0.01	0.04	0.05	0.76	0.01	0.10	0.11
Central Arctic Ocean	BN09	2.38	2.30	1.19	0.01	0.04	0.05	0.51	0.01	0.08	0.09
Central Arctic Ocean	BN10	2.42	2.40	1.28	0.01	0.14	0.15	2.02	0.09	0.49	0.48
Central Arctic Ocean	BN12	1.52	1.45	0.71	0.01	0.03	0.11	0.74	0.01	0.14	0.10
Central Arctic Ocean	BN13	2.87	2.29	1.14	0.01	0.03	0.06	0.43	0.01	0.07	0.07
Average		3.11	2.91	1.52	0.02	0.09	0.12	1.44	0.03	0.22	0.28
Average of the cruise		5.20	6.79	4.38	0.08	0.47	0.70	6.24	0.52	1.13	1.51

Location	Site	Chry	BaA	BbF	BkF	BaP	IP	DBahA	BghiP	Sum
Bering Sea	B02	2.44	0.41	2.25	0.12	0.26	0.37	0.33	1.55	34.51
Bering Sea	B04	4.63	0.77	3.67	0.67	1.16	0.64	0.49	3.79	46.30
Bering Sea	B06	4.40	0.77	4.26	0.19	0.73	0.70	0.57	3.80	51.15
Bering Sea	B07	1.97	0.28	1.45	0.07	0.22	0.20	0.21	0.99	26.21
Average		3.36	0.56	2.91	0.26	0.59	0.48	0.40	2.53	39.54
Bering Strait	B14	1.56	0.28	2.16	0.27	0.28	0.56	0.20	1.32	16.90
Bering Strait	BB06	1.26	0.25	1.31	0.15	0.19	0.30	0.16	0.93	16.08
Bering Strait	NB04	1.48	0.32	2.72	0.26	0.30	0.59	0.22	1.48	25.83
Bering Strait	NB08	0.43	0.47	0.89	0.08	0.08	0.12	0.07	0.35	8.45
Average		1.18	0.33	1.77	0.19	0.21	0.39	0.16	1.02	16.82
Chukchi Sea Shelf	SR01	0.80	0.15	0.97	0.10	0.13	0.20	0.16	0.60	8.76
Chukchi Sea Shelf	SR04	2.22	0.43	2.54	0.18	0.31	0.50	0.25	1.73	27.74
Chukchi Sea Shelf	SR05	3.01	0.58	3.19	0.28	0.45	0.64	0.30	2.21	58.02
Chukchi Sea Shelf	R08	5.68	1.37	4.19	0.33	0.77	0.70	0.46	2.59	63.88
Chukchi Sea Shelf	R09	3.93	0.73	2.82	0.24	0.49	0.58	0.36	2.41	46.37
Chukchi Sea Shelf	SR10	3.81	0.66	3.23	0.30	0.48	0.68	0.37	2.56	47.55
Chukchi Sea Shelf	SR11	8.33	1.31	7.00	0.63	0.93	1.44	0.78	5.22	78.33
Chukchi Sea Shelf	C07	5.27	0.94	3.71	0.35	0.71	0.76	0.46	3.20	75.76
Chukchi Sea Shelf	C09	4.22	0.79	3.24	0.30	0.62	0.74	0.43	2.83	45.07
Chukchi Sea Shelf	M07	3.66	0.40	3.29	0.22	0.19	0.42	0.28	0.94	44.62
Chukchi Sea Basin	M02	1.98	1.72	1.45	0.13	0.15	0.40	0.23	1.10	28.64
Chukchi Sea marine bench edge	BN03	5.79	0.93	10.82	1.59	0.92	4.69	1.41	9.30	71.81
Average		4.06	0.83	3.87	0.39	0.51	0.98	0.46	2.89	49.71
Northwind ridges	MOR02	5.11	0.65	5.85	0.75	0.52	2.45	0.84	7.22	58.88
Canadian Basin	MS02	4.74	0.59	4.08	0.54	0.38	0.81	0.44	2.92	70.49
Canadian Basin	S26	5.37	0.53	4.60	0.33	0.25	0.54	0.36	1.58	75.49
Average		5.08	0.59	4.85	0.54	0.39	1.27	0.55	3.91	68.29
Central Arctic Ocean	BN04	2.28	0.25	3.16	2.94	0.19	1.07	0.48	2.39	33.85
Central Arctic Ocean	BN06	0.41	0.07	0.69	0.35	0.20	0.32	0.11	0.28	13.26
Central Arctic Ocean	BN07	0.21	0.03	0.50	0.05	0.02	0.19	0.07	0.24	9.66
Central Arctic Ocean	BN09	0.17	0.04	0.46	0.11	0.02	0.39	0.08	0.25	8.21
Central Arctic Ocean	BN10	0.81	0.24	1.21	0.20	0.17	0.27	0.12	0.34	12.86
Central Arctic Ocean	BN12	0.12	0.03	0.62	0.02	0.02	0.06	0.03	0.06	5.79
Central Arctic Ocean	BN13	0.09	0.03	0.57	0.02	0.02	0.06	0.03	0.05	7.84
Average		0.58	0.10	1.03	0.53	0.09	0.34	0.13	0.52	13.07
Average of the cruise		2.87	0.53	2.90	0.39	0.37	0.71	0.35	2.14	37.28

534 **Table 2.** Summary of Σ_{18}PAHs concentrations (ng g^{-1} d.w.) in the surface sediment of
535 the Bering Sea, Bering Strait, Chukchi Sea, Canadian Basin and Central Arctic Ocean
536 for CHINARE 4 expedition.

	Range	Median	Mean	S.D.
Bering Sea	26.2-51.2	40.4	39.5	11.3
Bering Strait	8.5-25.8	16.5	16.8	7.1
Chukchi Sea	8.8-78.3	47.0	49.7	21.2
Canadian Basin	58.9-75.5	70.5	68.3	8.5
Central Arctic Ocean	5.8-33.9	9.7	13.1	9.6
Entire Cruise	5.8-78.3	34.2	37.3	24.0

537

538

539 **Table 3.** PAH variance explained and loadings of three significant factors by source
540 apportionment PCA analysis.

	Factor 1	Factor 2	Factor 3
Donations	32%	29%	27%
Fluor	.823	.429	.291
Py	.807	.397	.359
Flu	.805	.495	.042
BaP	.784	.163	.502
BaA	.703	.251	.270
Chry	.665	.544	.477
Acl	.654	.650	.357
Ant	.430	.145	-.136
Nap	.195	.943	.152
twoMN	.330	.912	.204
oneMN	.408	.873	.237
Ace	.631	.728	.200
Phe	.581	.695	.297
IP	.121	.081	.951
DBahA	.373	.231	.889
BghiP	.405	.181	.867
BbF	.402	.354	.820
BkF	-.216	.168	.736

541